EPJ Web of Conferences **40**, 13003 (2013)
DOI: 10.1051/epjconf/20134013003

Magnetic dispersion in a soft amorphous layer with a helical anisotropy profile

M. Gloanec[1], S. Dubourg[1], O. Acher[2], F. Duverger[1], D. Plessis[1] and A. Bonneau-Brault[1]

[1]CEA, DAM, Le Ripault, Laboratoire des Matériaux Magnétiques et Optiques, 37260 Monts, France
[2]HORIBA Jobin Yvon S.A.S., 5, rue Arago, 91380 Chilly Mazarin, France

Abstract. A new analysis method of the magnetization dispersion in a thin magnetic film is presented. It is based on the angular measurement of the permeability spectra and on the evaluation of the integral relation. It provides the average orientation of the magnetization in the layer and a dispersion parameter which quantifies the magnetic dispersion. The method is successfully applied on a soft CoNbZr 800nm magnetic layer which possesses a helical anisotropy profile. This helical profile is obtained by rotating continuously the sample during the sputtering deposition on a scale from R = 0 to 16 turns. The study reveals that, for about 1/2 turn, a maximal dispersion is achieved and, for more elevated rotation speed, the magnetization no longer follows the anisotropy profile but lines up along an easiest axis direction. The experimental data are well described by a one-dimensional micromagnetic model which takes both exchange coupling and a helical anisotropy into account. The analytical cases with an exchange constant null and infinite are also considered in order to gain more insight onto the observed magnetic behaviour in the soft magnetic thin film.

1 Introduction

Soft ferromagnetic thin films possess high permeability levels, a magnetic property which is largely used in lots of high frequency applications such as planar inductance, microwave filters or antiheft devices. The potentialities of the soft ferromagnetic materials can be evaluated by the generalized Snoek's law and the integral criterion equation. The former describes the existence of a trade-off between high permeability levels and high operating frequencies, while the latter establishes that the integral of $\mu'' \ f \ df$ is bounded by the square of saturation magnetization multiplied by a constant [1,2].

A challenge for microwave devices is to achieve magnetic materials whose properties can be tuned over a frequency band. Most of investigations are lead to increase the anisotropy of thin ferromagnetic layers or multilayers in order to acquire an elevated operating frequency. Fewer studies report on the decrease of the anisotropy, a case for which high permeability could be expected. One way consists in applying a rotating static magnetic field during annealing [3]. This treatment type can induce a drastic diminution of the effective anisotropy by randomizing the anisotropy axis. Another way is to use two crossed-anisotropy layers or to generate a domain-wall in a sandwiched-ferromagnet [4,5]. These last two systems have revealed unusual behaviors.

In this paper, we present an investigation of the dynamic magnetic properties of a soft layer with a helical anisotropy. A continuous rotation of the sample during the sputtering deposition allows achieving the helical anisotropy profile. The system acts as a model system to study the magnetization dispersion induced by the profile. A generalized analysis method to characterize this dispersion is shown. It is based on the angular evaluation of the integral criterion [6]. In contrast to the method recently proposed by Dubuget *et al*. [4], the analysis here is based on the whole permeability spectra and no particular law of magnetization dispersion is required. The method proposed here gives the average orientation of the magnetization and a dispersion parameter D which quantifies the magnetization dispersion. The results are compared with a one-dimensional (1D) micromagnetic model which simulates the static state of the magnetization in the thickness of a helical anisotropy sample and the associated microwave permeability spectra.

2 Experimental details

Thin magnetic layers were prepared with the nominal composition $Co_{86}Nb_{10.5}Zr_{3.5}$ by sputtering deposition under an Ar atmosphere (5×10^{-3} mbar). The deposition onto 9-mm-diameter glass substrate was with a rate of 8 nm/s and a base pressure lower than $1.5.10^{-6}$ mbar. A motorized goniometer allowed a continuous in-plane rotation of the sample during sputtering. Keeping the layer thickness constant at approximately 800 nm, the samples were rotated on a scale from R = 0 to 16 turns. When the growth started, an in-plane easy axis was induced in a direction y by the magnetron field of the cathode, while the reference direction is along a x axis.

For each in-plane orientation ϕ of the sample from the reference direction, complex permeability spectra measurements were performed from 10 MHz to 6 GHz by a single coil perturbation technique. The measurement setup and procedure are described elsewhere [6].

3 Generalized analysis method of the dispersion

In the polar coordinate system, we design by $m(\theta)d\theta$ the matter fraction with a magnetization orientation between θ and $\theta + d\theta$. $m(\theta) = m(\theta + 2\pi)$ is a periodic function which could be developed into Fourier series:

$$m(\theta) = \frac{1}{\pi}\left[\frac{1}{2} + \sum_{n=1}^{\infty} a_n \cos(n\theta) + b_n \sin(n\theta)\right] \qquad (1)$$

where

$$a_n = \int_0^{2\pi} m(\theta)\cos(n\theta)d\theta,\ \ b_n = \int_0^{2\pi} m(\theta)\sin(n\theta)d\theta,$$

and $\int_0^{2\pi} m(\theta)d\theta = 1$.

The complex permeability $\mu_h(\theta,f)$ of the fraction $m(\theta)d\theta$ along its hard axis at a frequency f can be expressed as a linear combination of Bloch-Bloemberger permeability expression. It can be shown that [2]:

$$\int_0^F \mu_h''(\theta,f)fdf \approx \frac{\pi}{2}\left(\bar{\gamma}4\pi M_S\right)^2 \qquad (2)$$

where F is the upper integral boundary large enough compared to the resonance frequency used in $\mu_h(\theta,f)$, $\gamma = 2\pi\bar{\gamma}$ is the gyromagnetic ratio and M_S the saturation magnetization.

The microwave permeability $\mu(\phi,f)$ on the whole sample evaluated along the direction ϕ can be written as :

$$\mu(\phi,f) \approx \int_0^{2\pi} m(\theta)\mu_h(\theta,f)\sin^2(\phi-\theta)d\theta. \qquad (3)$$

By using Eqs. (1), (2), (3), the microwave permeability integral on the whole sample

$I(\phi) \approx \int_0^F \mu''(\phi,f)fdf$ evaluated along the direction ϕ

could be easily deduced :

$$I(\phi) \approx I_{\max}\left[1 - a_2\cos(2\phi) - b_2\sin(2\phi)\right]/2. \qquad (4)$$

$I_{\max} = \frac{\pi}{2}\left(\bar{\gamma}4\pi M_S\right)^2$, a_2 and b_2 can be experimentally obtained with:

$$I_{\max} = I(0°) + I(90°),$$

$a_2 = [1\text{-}2\ I(0°)/I_{\max}]$ and, (5)

$b_2 = [1\text{-}2\ I(45°)/I_{\max}]$.

The quantity $D = \sqrt{a_2^2 + b_2^2}$ is a magnetization dispersion criterion. In the case of a pure uniaxial system, $m(\theta)$ is a Dirac function and D equals unity. On the other hand, the dispersion criterion D is null in the case of an isotropic system since $m(\theta)$ is a constant.

Hence, by the fitting of the experimental curve $I(\phi)$ it is possible to determine the average orientation of the magnetization and to quantify the angular magnetic dispersion in the sample.

4 Results

Figure 1 shows the imaginary part μ'' of the complex permeability spectra for the 0-turn sample measured at different orientations ϕ with respect to the reference axis. A maximum value of μ'' is observed at $\phi = 176°$ since the pumping field h_{RF} is normal to the magnetization direction. For $\phi = 86°$, no signal is measured given that h_{RF} is along a well-defined easy axis.

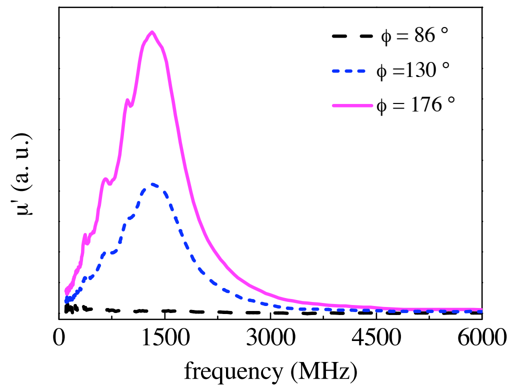

Fig. 1. *Imaginary part of the permeability spectra measured for the 0-turn sample along different orientations ϕ.*

Examples of the $I(\phi)/I_{\max}$ curves obtained on the 0- and 1/2-turn samples are displayed on the Figure 2. For the 0-turn sample, the minimum of $I(\phi)/I_{\max}$ is observed at $\phi = 86°$ in agreement with an easy axis direction expected along the y axis. The amplitude of $I(\phi)/I_{\max}$ reaches a maximum for this sample indicating a well-defined uniaxial anisotropy. The associated parameter dispersion D = 0.98 is then close to unity. On the other hand, the sample which has been continuously 1/2 turn rotated during sputtering deposition, shows a drastic decrease of the amplitude of $I(\phi)/I_{\max}$ and an angular shift of the minimum measured at 171°. The former indicates a strong dispersion and provides D = 0.3. The latter gives an average orientation of the magnetization that has shifted of about 90° in comparison with the 0-turn sample in agreement with the one expected for a helical anisotropy on an angular range of 180°.

The evolution of the experimental dispersion criterion D and the easiest axis orientation ϕ_{EA} as a function of the turn number R is plotted in Fig. 3 (black round symbols). First, D diminishes drastically from 0 to 1/2 turn, indicating an increase of the magnetization dispersion due to the helical anisotropy profile induced during sputtering. Beyond R =1/2 turn, D tends toward unity with slight oscillations. Consequently, the maximal randomization of the magnetization is achieved for 1/2 turn. For higher speed rotation during the layer growth, the magnetization no longer follows the anisotropy axes but prefers to line up along a direction which minimizes the energy and corresponds to the easiest axis ϕ_{EA}. This one oscillates as a function of the turn fraction as observed in Fig. 3 b.

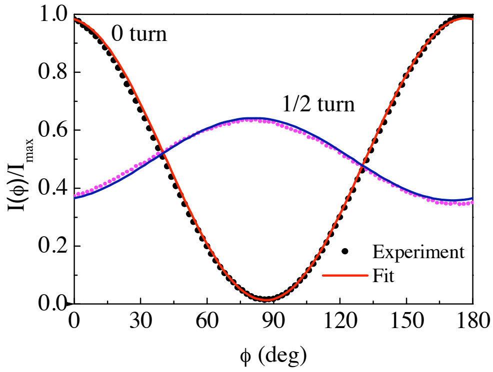

Fig. 2. *Experimental curves of $I(\phi)/I_{max}$ and associated fit for the 0-turn and 1/2-turn samples.*

We have compared the experimental data to one-dimensional (1D) micromagnetic calculations. The 1D model assumes a helical profile for the anisotropy into the layer thickness. Hence the orientation θ_K of the anisotropy axis is a linear function of the position z into the thickness t while the associated anisotropy constant remains unchanged $K(z) = K$. Following Ref. 4, the total micromagnetic energy density can be written as:

$$E = \frac{1}{t}\int_0^t \left\{ A_{ex}\left(\frac{d\theta}{dz}\right)^2 + K\sin^2[\theta(z) - \theta_K(z)] \right\} dz, \qquad (6)$$

where A_{ex} is the exchange constant and θ is the magnetization orientation. From the calculations of the static magnetization profiles, we could simulate the complex permeability spectra and deduce the D and ϕ_{EA} theoretical values for each turn number by using the procedure described in part 3. These theoretical curves are displayed in Fig.3. The parameters used for the calculations are a saturation magnetization M_S = 900 emu/cm^3, an exchange constant A_{ex} = 1.10^{-6} erg/cm [7], an anisotropy field $H_{K0} = 2K/M_S$ = 15 Oe (a value found in magnetometry), a thickness t = 800 nm, a gyromagnetic ratio $\bar{\gamma}$ = 3 MHz.Oe^{-1}, a damping parameter α = 0.015 and taking the skin effect into account, a resistivity ρ = 140.10^{-8} Ω m, a value expected for amorphous CoNbZr. The theoretical curves (straight red lines) reproduce well the behaviour of the magnetization as a function of the turn number: the maximum dispersion is found for a rotation of about 1/2 turn, D tends to unity for elevated turn number and oscillations occur. The easiest axis variations are also quite well described.

To gain more insight into this behaviour, we can consider the two analytical cases of A_{ex} = 0 and ∞. In the A_{ex} = 0 case (blue dashed lines in Fig. 3), the magnetization orientation follows perfectly the anisotropy profile. By using Eqs. (1) and (5), we can obtain the following relations :

$$a_2 = \frac{1}{4\pi R}\sin\{4\pi[R - trunc(R)]\},$$
$$b_2 = \frac{1}{4\pi R}(1 - \cos\{4\pi[R - trunc(R)]\}) \text{ and,} \qquad (7)$$
$$D = \frac{|\sin(2\pi R)|}{2\pi R},$$

where trunc (R) is the integer part of the turn number R. The $\sin_c$ variation of D explains the drastic drop of D for low turn number and the slight oscillations observed at high turn number. This behaviour characterizes the one of "thick" films in comparison with a Bloch wall $\pi(A_{ex}/K)^{1/2}$ ≅380 nm.

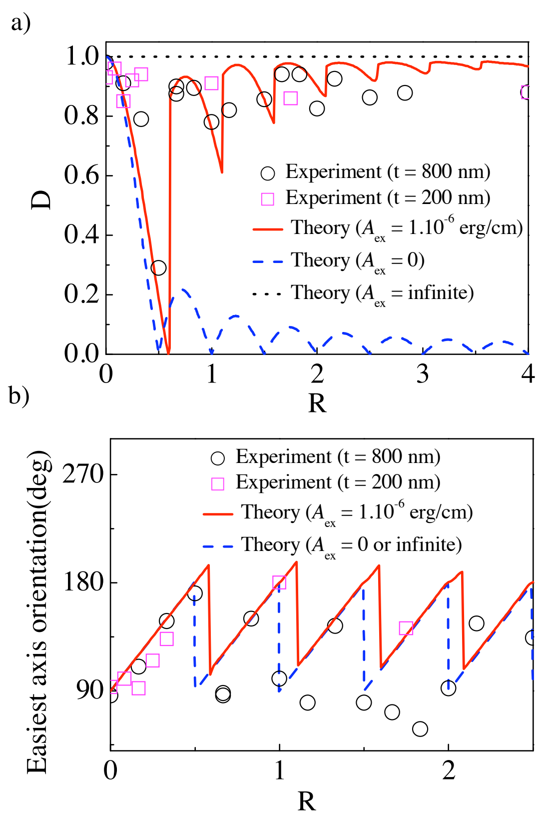

Fig. 3. *Experimental and theoretical D (a) and ϕ_{EA} (b) curves as a function of the turn number.*

In the infinite A_{ex} case, the magnetization is uniform into the layer thickness, the magnetic system is uniaxial and D equals unity. The magnetization behaviour describes then the one of "thin" films. The total magnetic energy density can be written as:

$$E = \int_{\pi/2}^{\pi/2+2\pi R} \left[\frac{K}{2\pi R} \sin^2(\theta - \theta_K) \right] d\theta_K \\ = K \frac{\sin(2\pi R)}{2\pi R} \cos^2(\theta - \pi R). \tag{8}$$

This expression approaches the one of a uniaxial system possessing an anisotropy constant K_{eff} = K $|\sin(2\pi R)|/(2\pi R)$ and an easiest axis direction which jumps every 1/2 turn. Note that exchange induces a small delay of the first ϕ_{EA} jump and the maximal randomization. The case of a thin CoNbZr film (t = 200 nm) in comparison with the Bloch wall is illustrated experimentally in Fig.3 (pink symbols). For this sample, the D parameter never drops toward 0 while the easiest axis varies between 90° and 180° as expected.

5 Conclusion

A new method has been presented to investigate the magnetization dispersion which is generated here by the anisotropy profile. Based on the angular measurement of the integral criterion, it requires no particular law of magnetization distribution. The main assumption is that the matter fraction with an infinitesimal magnetization orientation is a periodic function which can be described by a Fourier series. A D dispersion parameter quantifying the magnetization dispersion (isotropic and uniaxial behaviors for D = 0 and 1, respectively) and an easiest axis orientation can be deduced.

References

1. O. Acher and A. L. Adenot, Phys. Rev. B **62**, 11324 (2000)
2. O. Acher and S. Dubourg, Phys. Rev. B **77**, 104440 (2008)
3. K. Suzuki, N. Ito, J. S. Garitaonandia, and J. D. Cashion, J. Appl. Phys. **99**, 08F114 (2006).
4. V. Dubuget, A. Thiaville, F. Duverger, S. Dubourg, O. Acher, and A.-L. Adenot-Engelvin., Phys. Rev. B **80**, 134412 (2009)
5. F. Hagedorn, J. Appl. Phys. **40**, 5179 (1969)
6. M.Gloanec, S. Dubourg, O. Acher, F. Duverger, D. Plessis, A. Bonneau-Brault, Phys. Rev. B **85**, 094433 (2012)
7. A. Yoshihara, K. Takanashi, M. Shimoda, O. Kitakami, and Y. Shimada, Jpn. J. Appl. Phys. **33**, 3927 (1994)